BIOPHYSICS LETTER



An estimate to the first approximation of microtubule rupture force

Sharyn A. Endow¹ · Piotr E. Marszalek²

Received: 1 October 2018 / Revised: 18 February 2019 / Accepted: 17 May 2019 © European Biophysical Societies' Association 2019

Abstract

Microtubule mechanical properties are essential for understanding basic cellular processes, including cell motility and division, but the forces that result in microtubule rupture or breakage have not yet been measured directly. These forces are essential to understand the mechanical properties of the cytoskeleton and responses by cells to both normal conditions and stress caused by injury or disease. Here we estimate the force required to rupture a microtubule by analyzing kinesin-14 Ncd motor-induced microtubule breakage in ensemble motility assays. We model the breakage events as caused by Ncd motors pulling or pushing on single microtubules that are clamped at one end by other motors attached to the glass surface. The number of pulling or pushing Ncd motors is approximated from the length of the microtubule bound to the surface and the forces produced by the pulling or pushing motors are estimated from forces produced by the Ncd motor in laser-trap assays, reported by others. Our analysis provides an estimate, to the first approximation, of~500 pN for the minimal force required to rupture a 13-pf microtubule. The value we report is close to the forces estimated from microtubule stretching/fragmentation experiments and overlaps with the forces applied by AFM in microtubule indentation assays that destabilize microtubules and break microtubule protofilaments. It is also consistent with the forces required to disrupt protein noncovalent bonds in force spectroscopy experiments. These findings are relevant to microtubule deformation and breakage caused by cellular tension in vivo.

Keywords Microtubules Rupture force Kinesin-14 motor Motor force generation Microtubule gliding assays

Introduction

Migrating cells show large changes in cytoskeletal dynamics at the leading edge that cause microtubules growing towards the leading edge to buckle and break. The microtubule breakage is thought to be caused by assembly of new actin filaments at the leading edge, which produces both anterograde actin flow and coupled retrograde actin flow, driven by cytoplasmic myosin (Wang 1985; Lin et al. 1996)—the convergence of the forward and rearward actomyosin flow is hypothesized to produce sufficient mechanical strain on

Electronic supplementary material The online version of this article (https://doi.org/10.1007/s00249-019-01371-6) contains supplementary material, which is available to authorized users.

- * Sharyn A. Endow endow@duke.edu
- Department of Cell Biology, Duke University Medical Center, Durham, NC 27710, USA
- Department of Mechanical Engineering, Pratt School of Engineering, Duke University, Durham, NC 27708, USA

microtubules at the leading edge that it can cause them to break (Waterman-Storer and Salmon 1997; Gupton et al. 2002). Responses by the cell to basic processes, such as cell motility, thus rely on understanding the mechanical properties of microtubules.

The mechanical properties of microtubules have been studied extensively using a variety of experimental approaches, including mechanical manipulation of microtubules with laser tweezers (Kurachi et al. 1995), micropipette aspiration of microtubule-containing vesicles (Elbaum et al. 1996), and deformation of microtubules supported at their termini with an AFM tip (Kis et al. 2002). These studies resulted in the determination of basic elastic properties of microtubules, such as the Young's and shear moduli, e.g. (Kis et al. 2002), and produced a number of other interesting observations regarding the mechanical behavior of microtubules. More recently, the Young's modulus of microtubules was accurately determined in the absence of shear—this was elegantly done by performing tensile fragmentation tests of microtubules attached to a polydimethylsiloxane (PDMS) elastomer sheet that was coated with kinesin (Kabir et al.

Published online: 27 May 2019

2014). This latter approach could, in principle, also be used to estimate the tensile strength of individual microtubules (this point will be discussed later).

However, the forces that lead to individual microtubule rupture have not as yet been measured directly. Ideally, a single microtubule would be coupled to both a surface and a force-measuring device, such as an AFM cantilever, and the tensile force at rupture would be directly measured. However, such an approach would require a single microtubule to be coupled to the device through handles or chemical bonds that must themselves be stronger than microtubules, which have not been innovated so far. More typically, microtubules are coupled to force applying or measuring devices through numerous weak bonds distributed along the microtubule length, e.g., kinesin motors (Kabir et al. 2014) or antibodies. However, numerous attachments at the microtubule surface may themselves affect the mechanical strength of microtubules, as shown recently (Kabir et al. 2014). In addition to the lack of appropriate handles that are stronger than microtubules, direct measurement of microtubule breakage is hampered by the difficulty of identifying breakage events, rather than microtubule detachments or slippage.

Information regarding microtubule rupture forces is essential to understand the mechanical properties of the cytoskeleton, as well as basic biological processes such as cell motility, as mentioned previously, or division, in which a large number of motors and other proteins produce force to assemble microtubules into spindles, mediate chromosome congression to the metaphase plate, and separate half-spindles (Inoué and Salmon 1995). This information is also needed to understand the mechanics of proteins that severe microtubules and remodel the cytoskeleton during the cell cycle and in development, although severing proteins, e.g., katanin (McNally and Vale 1993) and spastin (Roll-Mecak and Vale 2005) break microtubules enzymatically, rather than mechanically.

Among the reports of microtubule breakage not due to severing proteins is microtubule breakage caused by the kinesin-14 Ncd motor protein in ensemble motility assays (Endow and Higuchi 2000). Ncd is a nonprocessive kinesin motor protein that hydrolyzes ATP, producing force to move along microtubules, but, unlike kinesin-1, Ncd detaches from microtubules after each ATP hydrolysis (Pechatnikova and Taylor 1999; Endow and Higuchi 2000). The working stroke of Ncd is a large rotation of the α -helical coiled-coil stalk (Yun et al. 2003) that displaces the motor towards the microtubule minus end (Endow and Higuchi 2000). A single mutation at the Ncd neck-stalk junction permits rotation by the stalk in either direction, causing the motor to move towards either the microtubule plus or minus end in gliding assays (Endow and Higuchi 2000). When assayed with polarity-labeled microtubules, the bidirectional Ncd motor showed gliding first in one direction and then the opposite

direction. The directional gliding and reversals of direction have been attributed to cooperativity of the Ncd motors bound to the microtubules (Sciambi et al. 2005). Microtubule breakage occurred sporadically during the assays, presumably caused by different regions of Ncd motors attached to the coverslip producing oppositely directed forces on the bound microtubules.

Here, we analyze kinesin-14 Ncd motor-induced microtubule breakage to obtain a first-approximation estimate of microtubule rupture force. We take into account microtubule binding by Ncd motors to the coverslip in the ensemble gliding assays, force produced by Ncd in laser-trap assays (Furuta et al. 2013), and noncovalent hydrogen-bonds between α,β -tubulin (α,β -Tub) subunits in a high-resolution cryoelectron microscopy (cryoEM) microtubule model (Zhang et al. 2018).

Materials and methods

Microtubule breakage

Videotapes of taxol-stabilized axoneme-microtubule (Ax-MT) complexes gliding on the kinesin-14 Ncd motor in ensemble motility assays were analyzed for microtubule breakage events. Gliding assays of Ncd fused at its N terminus to GST were performed in 10 mM NaPO₄ pH 7.4, 1 mM EGTA, 1 mM MgCl₂ and 5 mM Mg-ATP at 22 °C (Endow and Higuchi 2000). Ax-MT complexes were assembled by growing single microtubules from *Chlamydomonas* flagellar axonemes or axoneme doublets (Song et al. 1997). Estimates of the number of motors pulling or pushing on the microtubule at the time of rupture were made by measuring the microtubule length bound by Ncd motors attached to the coverslip in the videotaped sequences, as described in the text. Calibration of the videotaped images was performed by measuring a micrometer slide with 0.010 mm graduations imaged under the motility assay conditions. The calibration was confirmed by measuring P.angulatum striae (Sanderson 1990) imaged under the same conditions as the motility assays.

Estimates of force produced by Ncd

The geometry of the microtubules and Ncd motors in the gliding assays was modeled using measurements of microtubules and proteins from cryoEM and crystal structures to estimate the number of protofilaments bound by Ncd motors in the assays. The width of an α,β -Tub subunit was taken as approximately half its length, or $81.76 \text{ Å} * 0.5 = \sim 40.88 \text{ Å} = \sim 4.09 \text{ nm}$, calculated from a high-resolution cryoEM model of 13-protofilament (*pf*) microtubules with bound GDP (PDB 6DPV) (Zhang et al. 2018). The diameter (*d*) of a

13-pf microtubule formed by α , β -Tub dimers of ~ 4.09 nm length was obtained by d= circumference/ π = (~4.09 nm × 13 pf)/ π + ~4.09 nm= ~21 nm, with the ~4.09 nm added to adjust for taking the α , β -Tub width at the center rather than edge. Lengths for the motor-antibody complex were measured from crystal structures, giving Ab,~15 nm (Pease et al. 2008); GST,~3 nm (PDB 1UA5); Ncd stalk,~8 nm (PDB 1N6M); Ncd head beyond the stalk,~4 nm (PDB 1N6M).

Force produced by Ncd motors in ensemble motility assays was estimated from laser-trap data for force produced by 2-, 3- and 4-Ncd motor arrays joined by DNA linkers and spaced \sim 6 nm apart (Furuta et al. 2013). Motor number was plotted vs force from Fig. 3e inset (Furuta et al. 2013) and the data points were fit to a curve; the relationship between motor number (n) and force (f) produced by the Ncd motors was found to be f= 0.5 n - 0.47 pN (R= 0.998).

Microtubule structure

A near-atomic resolution cryoEM model of a microtubule with bound GDP (3.3 Å, PDB 6DPV) (Zhang et al. 2018) was analyzed in Chimera (Pettersen et al. 2004). Predicted longitudinal H-bonds between β -Tub (chain B) and α -Tub of the next adjacent α,β -Tub dimer (chain A) were identified in Chimera using *FindHBond* (Mills and Dean 1996) with *Relax H-bond constraints* and default relaxed tolerances of 0.4 Å and 20°. Predicted H-bonds in a near-atomic resolution cryoEM F-actin structural model (3.6 Å, PDB 5OOE) (Merino et al. 2018) were identified in the same way.

Results and discussion

Microtubules are formed by 12-16 protofilaments, each consisting of α,β-Tub dimers joined head-to-tail along the filament (Fig. 1a), which associate laterally with one another along their length. The α,β -Tub subunits in a protofilament and the protofilaments in a microtubule are held together by noncovalent bonds that include hydrogen-bonds (H-bonds), together with electrostatic, van der Waals and hydrophobic interactions. Because of the importance of H-bonds in folding and stability (Hubbard and Kamran Haider 2010; Pace et al. 2014), we analyzed the number of H-bonds between α,β-Tub subunits along a protofilament. Analysis of a nearatomic resolution cryoEM microtubule model (3.3 Å, PDB 6DPV) (Zhang et al. 2018) showed 8 predicted longitudinal H-bonds between adjacent α,β -Tub subunits in a protofilament, based on donor and acceptor proximity and geometry, and 3D distribution of complementary atoms (Mills and Dean 1996). The residues predicted to form H-bonds are depicted as space-filled models (Fig. 1b) and the H-bonds are shown in cyan (Fig. 1c) (Table 1).

Lateral interactions between protofilaments in near-atomic resolution cryoEM structures of microtubules in different nucleotide states (3.4–3.5 Å) consist of a single lock-and-key contact between adjacent α -Tub or adjacent β -Tub subunits that is similar in all nucleotide states (Zhang et al. 2015) (Fig. 1a). These lateral interactions contribute to the overall mechanical strength of microtubules, but are estimated to be \sim fivefold weaker than longitudinal bonds, contributing -3.2 to -5.7 k_BT per dimer, compared to -18.5 to -27.8 k_BT per dimer for longitudinal bonds (Van-Buren et al. 2002). Because of their much lower contribution to microtubule structural integrity, lateral bonds are not included in our analysis. For simplicity, we also do not consider the contributions of other noncovalent bonds to microtubule mechanical strength.

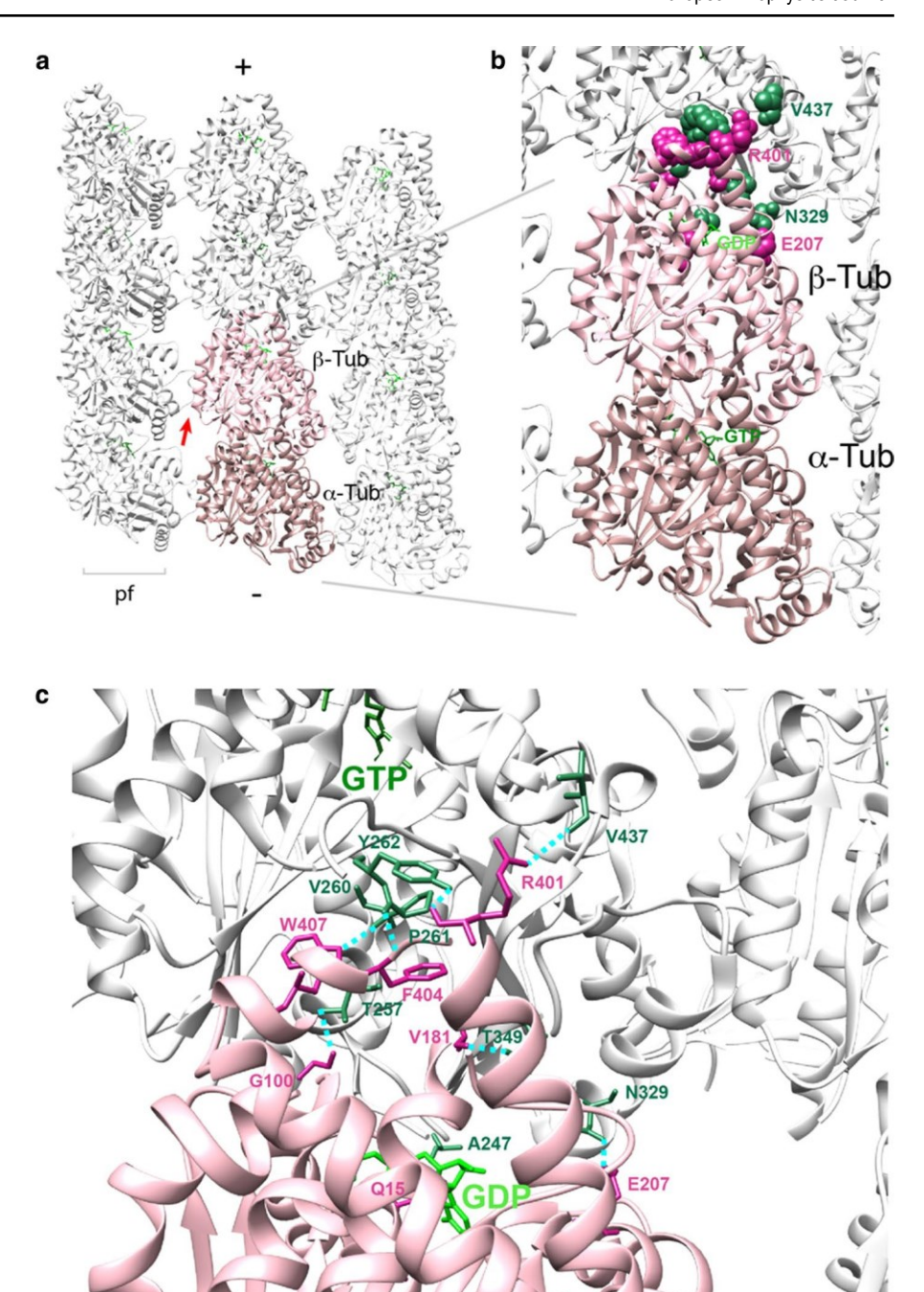
Microtubule breakage has been observed in ensemble motility assays (Song et al. 1997) of bidirectional kinesin-14 Ncd motors (Endow and Higuchi 2000) recorded by videoenhanced DIC (VE-DIC) (Inoué 1981; Allen et al. 1982). The microtubules in the gliding assays were grown from axonemes or axoneme doublets (Ax), which appear thicker than single microtubule (MTs) by VE-DIC. The majority of microtubules grown from axoneme doublets are 13-pf microtubules (90%) (Ray et al. 1993). Some of the Ax-MTs gliding on bidirectional Ncd motors in the assays were rotating as they glided, as reported previously for wild-type Ncd (Walker et al. 1990; Nitzsche et al. 2016). The gliding microtubules were observed at times to undergo buckling followed by rupture.

An example of a microtubule breakage is shown in Fig. 2 and Movie 1. The Ax-MT reversed direction three times prior to breaking, moving slowly at velocities of ~ 2–4 $\mu m/min$ in each direction, and was rotating, as indicated by the intermittent, slight lifting of the Ax doublet from the surface. It was gliding upward with the MT leading at the time of rupture. Just before rupturing, the Ax-MT paused (Fig. 2, frame 1), bulged slightly at or near the Ax-MT junction (Fig. 2, frame 2, arrow), then broke at the site of bulging (Fig. 2, frame 3). The bulging was interpreted to be caused by torsional effects due to the rotation. After breaking, the Ax and MT glided in opposite directions (Fig. 2, frame 4) with velocities of ~ 6.7 $\mu m/min$ and ~ 13.3 $\mu m/min$, respectively.

The Ax-MT complex appeared to be attached to the surface and was not moving during the 1–2 s prior to breaking. Because of this, we modeled the rupture as caused by Ncd motors pulling on a microtubule that was clamped to the coverslip surface by motors bound to the axoneme that were attempting to transport the microtubule in the opposite direction, causing it to break.

We measured the microtubule length that was bound to the coverslip just prior to the rupture to obtain an estimate of the number of Ncd motors bound to the microtubule during

Fig. 1 Microtubule structure. a Three protofilaments (pf) of a microtubule positioned vertically with the microtubule plus end (+) at the top (PDB 6DPV) (Zhang et al. 2018). An α,β-Tub dimer is highlighted in color (α-Tub, dark pink; β-Tub, pink; GTP, dark green; GDP, bright green). Lateral contact between β-Tub subunits in adjacent protofilaments (arrow). **b** α , β -Tub dimer showing residues (space-filled) predicted to form interdimer longitudinal H-bonds between β-Tub (magenta) and α-Tub of the next adjacent α,β -Tub dimer (dark green). Two residue pairs predicted to form H-bonds, V437-R401 and N329-E207, are labeled. c Predicted interdimer H-bonds (cyan; Table 1) between tubulin residues. One predicted H-bond (A247-Q15) is obscured by other residues and is not shown, and the donor F404 N atom in the F404-P261 H-bond is hidden behind another residue. Images rendered in Chimera (Pettersen et al. 2004)



the breakage. The length was 4.68 μ m for the microtubule part of the Ax-MT shown in Fig. 2. The number of motors bound to each protofilament of the microtubule was estimated by dividing the microtubule length by the length of an α,β -Tub dimer, 81.76 Å, calculated from a near-atomic resolution cryoEM model of a 13-pf microtubule bound to GDP (PDB 6DPV) (Zhang et al. 2018). This gave 572 α,β -Tub dimers per protofilament for the microtubule part of the Ax-MT in Fig. 2. There is one kinesin-binding site per α,β -Tub dimer (Hirose et al. 1995). Assuming that the binding sites are \sim 50% occupied, half the number of Ncd motors are bound to each protofilament. The Ncd motor in the gliding

assays was fused to glutathione-S-transferase (GST) and attached to anti-GST antibody bound to the glass surface. From the geometry and potential flexibility of the modeled Ncd motor-antibody complex (Fig. 3), the Ncd motor on the coverslip should be capable of binding to \sim 6 protofilaments of a 13-protofilament microtubule, giving \sim 1716 Ncd motors bound to the microtubule part of the Ax-MT in Fig. 2 at the time of rupture.

Force produced by Ncd has been measured in laser-trap assays of motors joined to one another by DNA scaffolds and found to be additive with increasing motor number (Furuta et al. 2013). The mean maximal force produced by 2-, 3- and

Table 1 Longitudinal H-bonds between α,β -Tub dimers in a protofilament

| Donor (D) | | | Acceptor (A) | | | D–A distance (Å) |
|-----------|---------|------|--------------|---------|------|------------------|
| Chain | Residue | Atom | Chain | Residue | Atom | |
| A | THR 257 | OG1 | В | GLY 100 | О | 3.212 |
| A | TYR 262 | OH | В | ARG 401 | O | 3.194 |
| A | ASN 329 | ND2 | В | GLU 207 | OE1 | 3.473 |
| A | THR 349 | OG1 | В | VAL 181 | O | 2.627 |
| *B | GLN 15 | NE2 | A | ALA 247 | O | 3.580 |
| В | ARG 401 | NH1 | A | VAL 437 | O | 3.482 |
| В | PHE 404 | N | A | PRO 261 | O | 3.058 |
| В | TRP 407 | NE1 | A | VAL 260 | O | 2.776 |

Predicted interdimer longitudinal H-bonds between adjacent α,β -Tub dimers in PDB 6DPV. Atoms are designated according to PDB conventions. Bonds are depicted in Fig. 1c, except the one marked with an asterisk

4-Ncd motor arrays spaced ~ 6 nm apart is ~ 0.55 pN, ~ 0.99 pN and ~ 1.55 pN, respectively [see Fig. 3e inset in (Furuta et al. 2013)]. The force, f, produced by n motors increases linearly as f = 0.5 n - 0.47 pN (R = 0.998), after curve-fitting analysis of the data in Fig. 3e inset. The force produced by the Ncd motors bound to the microtubule in Fig. 2 is estimated to be $(0.5 *\sim 1716 \text{ Ncd motors}) - 0.47 \text{ pN} = <math>\sim 858 \text{ pN}$.

Gliding assays of bidirectional Ncd motors (Endow and Higuchi 2000) resulted in a number of microtubule ruptures. Breakage events were analyzed in which the Ax-MT was attached to the surface along its length and was either paused or moving slowly at the time of breakage and in which the microtubule glided after breaking. These ruptures were modeled as due to Ncd motors pulling or pushing on a microtubule that was attached to an Ax or Ax-MT region that was clamped to the coverslip by other Ncd motors. The critical detachment force for single Ncd motors from microtubules has been estimated to be at least 2.0 pN and as high as 10 pN in laser-trap assays [Fig. S18C (Furuta et al. 2013)], which is greater by five- to seven-fold or more than the force produced by a single Ncd motor—this means that binding by Ncd can effectively clamp an Ax or Ax-MT to the coverslip surface. We excluded from our analysis microtubule ruptures in which the MT or Ax was not fully attached to the coverslip surface and the unattached part of the complex showed movement followed by breakage—these ruptures were attributed to viscous forces acting to bend or deform, then break the unattached microtubule region (n = 4).

The Ax-MT complexes that we analyzed are listed in Table 2. They show microtubule rupture forces of $\sim 300-3300$ pN, reflecting the different lengths of microtubules involved in the breakage events (total = 10). The lower values indicate the minimal forces needed for microtubule rupture, whereas the larger values arise from long microtubules that undergo breakage. The data indicate that forces as small as $\sim 300-700$ pN can break a microtubule under our assay conditions. The smallest forces that we observed are

 536 ± 181 pN (mean \pm SD, n = 4, total = 10). This gives ~ 500 pN as an estimate, to the first approximation, of the minimal force required to rupture a 13-pf microtubule.

Several factors could affect this estimate: 1) first, an assumption that we made in approximating microtubule rupture forces is that binding sites for Ncd on the microtubules were ~ 50% occupied, which may not be the case. However, this assumption is consistent with previously observed high on-rates for Ncd motors held close to a microtubule (Furuta et al. 2013), which is also likely to occur for microtubules binding to Ncd-coated coverslips in ensemble gliding assays. 2) We further assumed that all the bound motors were pulling or pushing at the same time and not stalled, based on findings for Ncd force production in laser-trap assays. This would be difficult to confirm in the ensemble gliding assays; however, variability in the number of pulling or pushing Ncd motors in the gliding assays could contribute to the relatively large standard deviation we observe for the smallest rupture forces. 3) A third assumption was that the absolute force produced by n motors increases linearly with the number of motors as f = 0.5n - 0.47 pN, based on curve-fitting analysis of previously reported laser-trap data (Furuta et al. 2013) this again assumes that all the bound motors are producing force and pulling or pushing at the same time. If the bound motors do not all produce force at the time of breakage, the forces during breakage would be overestimated. At the same time, if the Ncd motors in the gliding assays produce forces that are larger than those extrapolated from laser-trap assays of 2 to 4 Ncd motor arrays (Furuta et al. 2013), the forces during breakage would be underestimated. Taken together, the consequences of this assumption on our force estimates could counteract, effectively negating each other. 4) Finally, rotation of the Ax-MT complexes indicates that Ncd motors produce torque during motility (Walker et al. 1990; Endow and Higuchi 2000; Nitzsche et al. 2016), consistent with an off-axis Ncd working stroke (Hallen et al. 2011). This means that the mechanical failure of microtubules caused by strain

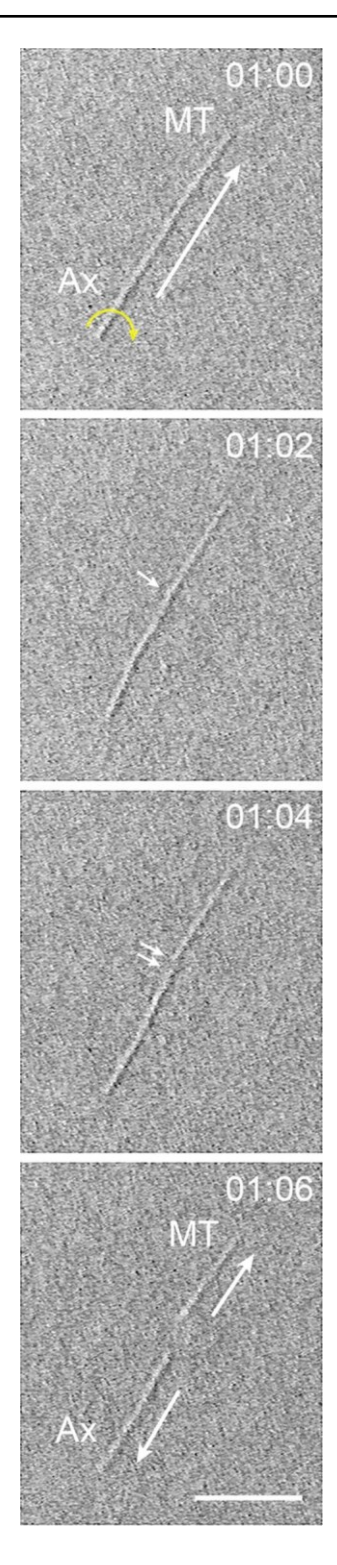
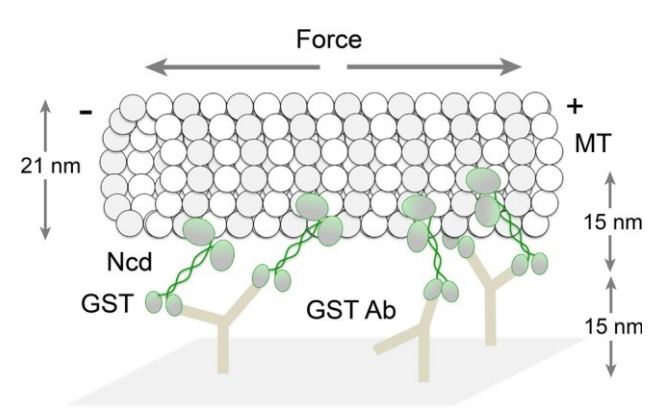


Fig. 2 Microtubule breakage in gliding assays of a bidirectional Ncd motor. Axoneme doublet (Ax, bottom) from which a single microtubule (MT, top) was grown; the slightly thicker Ax doublet is apparent in some images, but not others. Prior to rupturing, the Ax-MT moved slowly upward (frame 1, white arrow) and rotated (frame 1, yellow arrow). It paused, bulged slightly at or near the Ax-MT junction (frame 2, arrow), broke (frame 3, arrows), and the two parts glided in opposite directions (frame 4, arrows). See Movie 1. Time, min:sec. Bar, 5 μ m



Glass Surface

Fig. 3 Diagrammatic model of microtubule gliding assays. Microtubule (MT) gliding on Ncd fused to GST (both green-gray) bound to anti-GST antibodies (GST Ab, tan) attached to the glass surface (bottom, gray). The glass surface is coated with Ncd-Ab complexes in the assays with the bidirectional Ncd motors bound to the same site on α-β tubulin dimers of the microtubule (Hirose et al. 1995). Potentially flexible regions of GST-Ncd at the motor-stalk and stalk-GST junctions and at the GST Ab hinge region allow binding by Ncd to the lower~6 protofilaments of the microtubule. The bound Ncd motors produce force in opposite directions, presumably caused by rotation of the stalk towards the microtubule minus (left) or plus end (right) (Endow and Higuchi 2000). Motor cooperativity (Sciambi et al. 2005) would result in adjacent Ncd motors producing force in the same direction. The opposing forces produced by many bound Ncd motors are interpreted here to result in microtubule rupture. Protein dimensions estimated from cryoEM and crystal structures, as described in "Materials and methods". Drawing roughly to scale

produced by Ncd in gliding assays has a torsional component due to twisting, as shown previously for actin filament rupture (Tsuda et al. 1996).

The tensile strength of a single microtubule can also be estimated from the results of microtubule stretching/fragmentation tests reported by others (Kabir et al. 2014). Assuming the magnitude of the Young's modulus of a microtubule to be 12 MPa, the cross sectional area of a microtubule to be $\sim 4.9 \times 10^{-16}$ m², and the strain at which microtubules first fragment to be 4.28% (Kabir et al. 2014), our estimate of the force causing mechanical failure of microtubules in the stretching/fragmentation assays is ~ 250 pN, which is close to our smallest estimated microtubule rupture forces of 300–700 pN:

$$F = 12 \times 10^6 \text{ N/m}^2 \times 4.9 \times 10^{-16} \text{ m}^2 \times 0.0428 = 0.25 \times 10^{-9} \text{ N}$$

The estimated minimal mean force of ~ 500 pN required for rupturing a 13-pf microtubule that we obtained in this study implies that ~ 40 pN is required to break each protofilament—this is also expected to approximate the force required to dissociate an α,β -Tub subunit from a microtubule end. This is much greater than disassembly forces produced by the microtubule depolymerase kinesin-13 MCAK, where 1–2 motors producing ~ 1 pN each are capable of interacting

Table 2 Microtubule rupture forces

| Ax-MT | Ax or Ax- MT length (μm) ^a | MT length (μm) ^a | Force (pN) ^b | Ax-MT motility |
|-------|---|-----------------------------|-------------------------|--|
| 1 | 3.25 | 6.5 | 1192 | Slight movement with Ax leading, broke at Ax-MT junction, depolymerized in opposite directions at break |
| 2 | 5.85 | 7.15 | 1312 | MT leading, moving slowly, broke at Ax-MT junction, disassembled at break, two parts moved in opposite directions |
| 3A | 9.36 | 5.33 | 978 | Ax joined to two single MTs (A, B) moving with Ax leading, MT A broke, moved |
| 3B | 12.09 | 1.56 | 286 | upward; then MT B broke, moved slightly upward; Ax continued moving downward in opposite direction |
| 4 | 3.12 | 2.86 | 525 | Gliding with Ax leading, hit another Ax-MT gliding in opposite direction, paused for ~12 s, buckled, broke at or near junction, MT continued gliding in same direction, Ax bound to the Ax of the Ax-MT complex it hit and moved in opposite direction |
| 5 | 9.23 | 17.69 | 3246 | MT leading, moving slowly, a region of \sim 2.47 μm at Ax-MT junction buckled and broke, then disassembled, both parts moved in same direction |
| 6 | 7.93 | 18.21 | 3340 | MT leading, moving slowly, Ax stopped, broke at Ax-MT junction, Ax bound to other MTs, MT glided in same direction as before breaking |
| 7 | 10.40 | 3.51 | 643 | MT leading, broke in MT at start of imaging, both parts glided in same direction, broken Ax-MT slowed and curved |
| 8 | 8.45 | 3.77 | 691 | MT leading, moving slowly, broke in MT, MT glided down, broken Ax-MT stopped, then glided down more slowly |
| 9 | 6.50 | 4.68 | 858 | MT leading, moving slowly, rotating, paused, broke at Ax-MT junction, Ax and MT glided in opposite directions (Fig. 2 and Movie 1) |

^aLength of ruptured Ax, Ax-MT, or MT at time of break

with and dissociating α,β-Tub subunits from a microtubule end (Oguchi et al. 2011). However, microtubules can depolymerize spontaneously at their ends (Mitchison and Kirschner 1984), indicating that microtubule ends exist in an equilibrium between assembly and disassembly. MCAK and other kinesin-13 motors can disassemble microtubules by binding to the ends without hydrolyzing ATP and producing force (Moores et al. 2002; Hunter et al. 2003). This implies that binding by MCAK to microtubule ends is sufficient to shift the equilibrium towards disassembly, causing tubulin dimers to dissociate from the ends. Thus, the mechanism of kinesin-13-mediated dissociation of tubulin dimers from microtubule ends differs from microtubule rupture. An important difference is that microtubule rupture involves breakage of bonds between α,β-Tub subunits on more than one protofilament, differing from dissociation of α,β -Tub subunits from microtubule ends.

Microtubule deformation assays performed by AFM have provided estimates of forces required to indent a microtubule (Schaap et al. 2006), although the number of protofilaments that are deformed during the indentations is not certain. At higher forces than the ~ 300 pN used for the indentations, microtubule instability or breakage of the microtubule wall was observed (Schaap et al. 2006). The smallest forces of $\sim 300-700$ pN required for microtubule rupture that we observe in this study overlap with the forces of > 300 pN that cause protofilaments to break. Thus, the

first-approximation estimate of microtubule rupture force that we report here is consistent with forces applied previously to microtubules that destabilize microtubules and cause microtubule protofilaments to break.

Our estimated minimal microtubule rupture force implies that ~ 5 pN per H-bond can rupture the ~ 104 interdimer H-bonds predicted to form between α,β -Tub dimers in a 13-pf microtubule, given ~ 8 predicted longitudinal interdimer H-bonds/pf. This is fourfold lower than the ~ 20 pN per H-bond estimated to be required for actin filament rupture, based on rupture forces of ~ 400 pN measured using microneedles (Tsuda et al. 1996) and ~ 18 predicted lateral and longitudinal H-bonds between actin subunits in F-actin (PDB 5OOE) (Merino et al. 2018). However, it is roughly consistent with the ~ 10 –100 pN forces estimated by others to be required to break noncovalent bonds or interactions, e.g., from force spectroscopy measurements (Marszalek et al. 1999; Evans 2001; Bertz et al. 2010).

These forces contrast with the much higher forces of ~ 1000 –4000 pN required to break a single covalent bond (Grandbois et al. 1999). Generally, the measured strength of a bond, either covalent or noncovalent, refers to average stretching rates in single molecule force spectroscopy experiments (roughly 1 μ m/s for proteins) and depends logarithmically on the rate at which force is applied to the bond—the faster the stretching, the greater the rupture force. Under force clamp conditions, these bonds rupture at the given

^bForce = (((MT length/81.76 Å) × 6 × 0.5) × 0.5) – 0.47 pN

forces within an experimentally observable time, i.e., from milliseconds to seconds. For α,β -Tub dimer interactions in a 13-pf microtubule with ~ 104 H-bonds/MT, the minimal rupture force that we estimate of ~ 500 pN = ~ 5 pN/H-bond falls roughly into the predicted range of ~ 10–100 pN required to break noncovalent bonds or interactions, as noted above.

The minimal microtubule rupture force that we estimate here is sufficiently low to be produced by cytoskeletal motors in the cell, given that cytoplasmic microtubules are thought to contain arrays of different motors that produce force in the same or opposite direction, generating strain. It would be of interest to determine whether microtubule rupture is increased in cellular structures or regions in which large numbers of oppositely directed motors act on the same microtubules, e.g., spindle fibers during mitosis or axonal microtubules that form tracks for vesicle transport. Strain produced by the convergence of anterograde and retrograde actin or actomyosin flow at the leading edge of migrating cells has already been shown to cause breakage of microtubules at the leading edge (Waterman-Storer and Salmon 1997; Gupton et al. 2002). Microtubule rupture is also likely to occur during other cellular processes in which large changes in the cytoskeleton are accompanied by changes in force. These processes include remodeling of the microtubule cytoskeleton during spindle assembly prior to mitosis, anaphase separation of chromosomes and cytokinesis, and developmental events such as platelet activation, wound healing and dorsal closure in which cells or tissues undergo remodeling. Further investigation of microtubule rupture during these events would be of interest to determine the effects of mechanical strain on the cytoskeleton and the filaments that act to maintain cellular structure.

Acknowledgements This study was supported by US National Science Foundation Grant #CMMI-1660924 to SAE and #MCB-1517245 to PEM. Any opinions, findings, conclusions or recommendations expressed in this paper are those of the authors and do not necessarily reflect the views of the National Science Foundation. We thank Shin'ichi Ishiwata for valuable discussions.

Author contributions SAE designed the study, analyzed data, prepared figures and wrote the manuscript; PEM contributed to data analysis and interpretation, and manuscript writing.

Compliance with ethical standards

Conflict of interest The authors declare that they have no conflict of interest.

References

Allen RD, Metuzals J, Tasaki I, Brady ST, Gilbert SP (1982) Fast axonal transport in squid giant axon. Science 218:1127-1129
Bertz M, Chen J, Feige MJ, Franzmann TM, Buchner J, Rief M (2010) Structural and mechanical hierarchies in the

- alpha-crystallin domain dimer of the hyperthermophilic small heat shock protein Hsp16.5. J Mol Biol 400:1046–1056
- Elbaum M, Kuchnir Fygenson D, Libchaber A (1996) Buckling microtubules in vesicles. Phys Rev Lett 76:4078–4081
- Endow SA, Higuchi H (2000) A mutant of the motor protein kinesin that moves in both directions on microtubules. Nature 406:913–916
- Evans E (2001) Probing the relation between force lifetime and chemistry in single molecular bonds. Annu Rev Biophys Biomol Struct 30:105–128
- Furuta K, Furuta A, Toyoshima YY, Amino M, Oiwa K, Kojima H (2013) Measuring collective transport by defined numbers of processive and nonprocessive kinesin motors. Proc Natl Acad Sci USA 110:501-506
- Grandbois M, Beyer M, Rief M, Clausen-Schaumann H, Gaub HE (1999) How strong is a covalent bond? Science 283:1727–1730
- Gupton SL, Salmon WC, Waterman-Storer CM (2002) Converging populations of F-actin promote breakage of associated microtubules to spatially regulate microtubule turnover in migrating cells. Curr Biol 12:1891–1899
- Hallen MA, Liang Z-Y, Endow SA (2011) Two-state displacement by the kinesin-14 Ncd stalk. Biophys Chem 154:56–65
- Hirose K, Lockhart A, Cross RA, Amos LA (1995) Nucleotidedependent angular change in kinesin motor domain bound to tubulin. Nature 376:277–279
- Hubbard RE, Kamran Haider M (2010) Hydrogen bonds in proteins: role and strength. In: Encyclopedia of Life Sciences. John Wiley & Sons, Chichester, UK
- Hunter AW, Caplow M, Coy DL, Hancock WO, Diez S, Wordeman L, Howard J (2003) The kinesin-related protein MCAK is a microtubule depolymerase that forms an ATP-hydrolyzing complex at microtubule ends. Mol Cell 11:445–457
- Inoué S (1981) Video image processing greatly enhances contrast, quality, and speed in polarization-based microscopy. J Cell Biol 89:346–356
- Inoué S, Salmon ED (1995) Force generation by microtubule assembly/disassembly in mitosis and related movements. Mol Biol Cell 6:1619–1640
- Kabir AM, Inoue D, Hamano Y, Mayama H, Sada K, Kakugo A (2014) Biomolecular motor modulates mechanical property of microtubule. Biomacromol 15:1797–1805
- Kis A, Kasas S, Babic B, Kulik AJ, Benoit W, Briggs GA, Schonenberger C, Catsicas S, Forro L (2002) Nanomechanics of microtubules. Phys Rev Lett 89:248101
- Kurachi M, Hoshi M, Tashiro H (1995) Buckling of a single microtubule by optical trapping forces: direct measurement of microtubule rigidity. Cell Motil Cytoskel 30:221–228
- Lin CH, Espreafico EM, Mooseker MS, Forscher P (1996) Myosin drives retrograde F-actin flow in neuronal growth cones. Neuron 16:769–782
- Marszalek PE, Lu H, Li H, Carrion-Vazquez M, Oberhauser AF, Schulten K, Fernandez JM (1999) Mechanical unfolding intermediates in titin modules. Nature 402:100–103
- McNally FJ, Vale RD (1993) Identification of katanin, an ATPase that severs and disassembles stable microtubules. Cell 75:419–429
- Merino F, Pospich S, Funk J, Wagner T, Kullmer F, Arndt HD, Bieling P, Raunser S (2018) Structural transitions of F-actin upon ATP hydrolysis at near-atomic resolution revealed by cryo-EM. Nat Struct Mol Biol 25:528–537
- Mills JE, Dean PM (1996) Three-dimensional hydrogen-bond geometry and probability information from a crystal survey. J Comput Aided Mol Des 10:607–622
- Mitchison T, Kirschner M (1984) Dynamic instability of microtubule growth. Nature 312:237–242

- Moores CA, Yu M, Guo J, Beraud C, Sakowicz R, Milligan RA (2002) A mechanism for microtubule depolymerization by KinI kinesins. Mol Cell 9:903–909
- Nitzsche B, Dudek E, Hajdo L, Kasprzak AA, Vilfan A, Diez S (2016) Working stroke of the kinesin-14, ncd, comprises two substeps of different direction. Proc Natl Acad Sci USA 113:E6582–e6589
- Oguchi Y, Uchimura S, Ohki T, Mikhailenko SV, Ishiwata S (2011) The bidirectional depolymerizer MCAK generates force by disassembling both microtubule ends. Nat Cell Biol 13:846–852
- Pace CN, Fu H, Lee Fryar K, Landua J, Trevino SR, Schell D, Thurlkill RL, Imura S, Scholtz JM, Gajiwala K, Sevcik J, Urbanikova L, Myers JK, Takano K, Hebert EJ, Shirley BA, Grimsley GR (2014) Contribution of hydrogen bonds to protein stability. Protein Sci 23:652–661
- Pease LFI, Elliott JT, Tsai D-H, Zachariah MR, Tarlov MJ (2008) Determination of protein aggregation with differential mobility analysis: application to IgG antibody. Biotechnol Bioeng 101:1214–1222
- Pechatnikova E, Taylor EW (1999) Kinetics processivity and the direction of motion of Ncd. Biophys J 77:1003–1016
- Pettersen EF, Goddard TD, Huang CC, Couch GS, Greenblatt DM, Meng EC, Ferrin TE (2004) UCSF Chimera a visualization system for exploratory research and analysis. J Comput Chem 25:1605–1612
- Ray S, Meyhöfer E, Milligan RA, Howard J (1993) Kinesin follows the microtubule's protofilament axis. J Cell Biol 121:1083–1093
- Roll-Mecak A, Vale RD (2005) The *Drosophila* homologue of the hereditary spastic paraplegia protein, spastin, severs and disassembles microtubules. Curr Biol 15:650–655
- Sanderson JB (1990) The measurement of three light microscope test diatoms by scanning electron microscopy. Proceedings RMS 25:195–203
- Schaap IA, Carrasco C, de Pablo PJ, MacKintosh FC, Schmidt CF (2006) Elastic response, buckling, and instability of microtubules under radial indentation. Biophys J 91:1521–1531
- Sciambi CJ, Komma DJ, Sköld HN, Hirose K, Endow SA (2005) A bidirectional kinesin motor in live *Drosophila* embryos. Traffic 6:1036–1046

- Song H, Golovkin M, Reddy ASN, Endow SA (1997) In vitro motility of AtKCBP, a calmodulin-binding kinesin protein of Arabidopsis. Proc Natl Acad Sci USA 94:322–327
- Tsuda Y, Yasutake H, Ishijima A, Yanagida T (1996) Torsional rigidity of single actin filaments and actin–actin bond breaking force under torsion measured directly by *in vitro* micromanipulation. Proc Natl Acad Sci U S A 93:12937–12942
- VanBuren V, Odde DJ, Cassimeris L (2002) Estimates of lateral and longitudinal bond energies within the microtubule lattice. Proc Natl Acad Sci USA 99:6035–6040
- Walker RA, Salmon ED, Endow SA (1990) The *Drosophila claret* segregation protein is a minus-end directed motor molecule. Nature 347:780–782
- Wang YL (1985) Exchange of actin subunits at the leading edge of living fibroblasts: possible role of treadmilling. J Cell Biol 101:597-602
- Waterman-Storer CM, Salmon ED (1997) Actomyosin-based retrograde flow of microtubules in the lamella of migrating epithelial cells influences microtubule dynamic instability and turnover and is associated with microtubule breakage and treadmilling. J Cell Biol 139:417–434
- Yun M, Bronner CE, Park C-G, Cha S-S, Park H-W, Endow SA (2003) Rotation of the stalk/neck and one head in a new crystal structure of the kinesin motor protein, Ncd. EMBO J 22:5382–5389
- Zhang R, Alushin GM, Brown A, Nogales E (2015) Mechanistic origin of microtubule dynamic instability and its modulation by EB proteins. Cell 162:849–859
- Zhang R, LaFrance B, Nogales E (2018) Separating the effects of nucleotide and EB binding on microtubule structure. Proc Natl Acad Sci USA 115:E6191–e6200

Publisher's Note Springer Nature remains neutral with regard to jurisdictional claims in published maps and institutional affiliations.

3